IEICE TRANS. FUNDAMENTALS, VOL. E78–A, NO. 11 NOVEMBER 1995

PAPER

Performance of Single- and Multi-Reference NLMS Noise Canceller Based on Correlation between Signal and Noise

Yapi ATSE†, *Nonmember*, Kenji NAKAYAMA††, *and* Zhiqiang MA††, *Members*

SUMMARY Single-reference and multi-reference noise canceller (SRNC and MRNC) performances are investigated based on correlation between signal and noise. Exact relations between these noise canceller performances and signal-noise correlation have not been well discussed yet. In this paper, the above relations are investigated based on theoretical, analysis and computer simulation. The normalized LMS (NLMS) algorithm is employed. Uncorrelated, partially correlated, and correlated signal and noise combinations are taken into account. Computer simulation is carried out, using real speech, white noise, real noise sound, sine wave signals, and their combinations. In the SRNC problem, spectral analysis is applied to derive the canceller output power spectrum. From the simulation results, it is proven that the SRNC performance is inversely proportional to the signal-noise correlation as expected by the theoretical analysis. From the simulation results, the MRNC performance is more sensitive to the signal-noise correlation than that of SRNC. When the signal-noise correlation is high, by using a larger number of adaptive filter taps, the noise is reduced more, and, the signal distortion is increased. This means the signal components included in the noise are canceled exactly.

key words: *noise canceller, normalized LMS algorithm, signal-noise correlation, multi-reference noise canceller*

1. Introduction

Usually, noise canceller problem is investigated based on a single reference noise source. Unfortunately, in some practical applications, several noises may be propagated from different noise sources [1]–[3]. One typical consideration of interest is that of a computer room, where the speech of an operator may be corrupted by noises coming from several computers, such as workstations, and an air-conditioner. Usually, adaptation of the noise canceller is affected by the signal-noise correlation, and does not converge to the optimum solution. Therefore, the adaptation is stopped when the signal is received. However, relation between the signal-noise correlation and the noise canceller performance has not been well discussed. Recently, authors have investigated theoretically this relation, and have derived some mathematical relations [4], [5]. Based on this result, the noise canceller performance can be predicted to some extent.

The objective of this paper is to investigate relations between the correlation of the signal and the noise and noise cancellation in the cases of single reference and multi-reference noise cancellers (SRNC and MRNC). First, for the single-reference configuration, different combinations are used, namely single-frequency sine wave, multi-frequency sine wave, white noise, environment noise and speech signal. Second, based on these results, the multi-reference configuration can be investigated more easily. The noise canceller circuits are described in both configurations. The adaptive filter adjusting process is carried out by the normalized LMS (NLMS) algorithm.

2. Single-Reference Noise Canceller

2.1 Block Diagram

Figure 1 shows a block diagram of SRNC. The blocks F_1 and F_2 represent the transfer function of the noise paths. A transversal FIR adaptive filter is employed. Two adders are used to form the desired response $d(n)$, and the output of the canceller $e(n)$. The inputs of F_1 and F_2 are generated from the same noise source. The adaptive filter tap-weights are adjusted by using the NLMS algorithm.

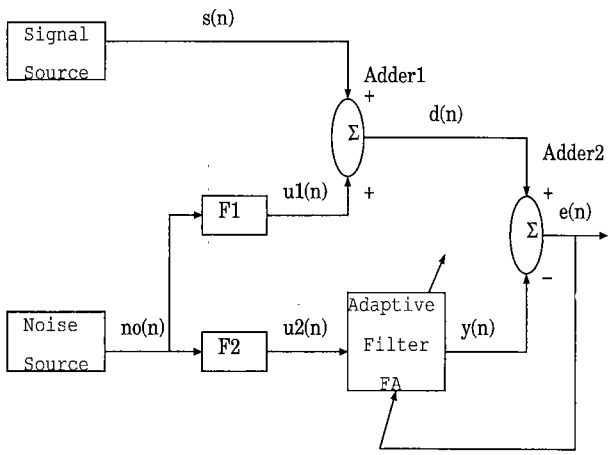

Fig. 1 Block diagram of single reference noise canceller.

Manuscript received May 30, 1994.
Manuscript revised April 17, 1995.

†The author is with the Faculty of Engineering, Kanazawa University, Kanazawa-shi, 920 Japan.
††The authors are with the Graduate School of Natural Science & Technology, Kanazawa University, Kanazawa-shi, 920 Japan.

2.2 Summary of Normalized LMS Algorithm

The NLMS algorithm is briefly summarized here [3]. Let $\mathbf{w}(n)$ be a tap-weight vector at iteration n.

$$\mathbf{w}(n) = [w_0(n), w_1(n), \cdots, w_{m-1}(n)]^T, \tag{1}$$

and $\mathbf{u}_2(n)$ be the adaptive filter input vector at iteration n,

$$\mathbf{u}_2(n) = [u_2(n), u_2(n), \cdots, u_2(n-M+1)]^T, \tag{2}$$

where T is the vector transposition. $\mathbf{w}(n)$ is adjusted following

$$\mathbf{w}(0) = \mathbf{0} \tag{3}$$

$$y(n) = \mathbf{w}(n)^T \mathbf{u}(n) \tag{4}$$

$$e(n) = d(n) - y(n) \tag{5}$$

$$\mu(n) = \frac{2\tilde{\mu}}{a + \sum_{k=1}^{k=M} u_2^2(n-k+1)} \tag{6}$$

$$\mathbf{w}(n+1) = \mathbf{w}(n) + \mu(n) e(n) \mathbf{u}(n) \tag{7}$$

where $\mathbf{0}$ denotes the null vector, $\mu(n)$ a time dependent step-size parameter, M the adaptive filter length, a a small positive constant, and $\tilde{\mu}$ a time independent step-size.

2.3 Mathematical Analysis of SRNC Performance

Theoretical analysis is carried out by applying a well familiar technique, spectral analysis to the noise canceller circuit. By doing so, mathematical formulas, all with their proofs, are derived. The analysis is carried out in the frequency domain, rather than in the time domain, for simplicity reason. Of course, the results obtained in the frequency domain can be transformed in the time domain.

The analysis consists in deriving the relationship between the canceller output power spectrum and the signal-noise cross-spectrum due to their cross-correlation. The adaptive filter is assumed to operate in a stationary environment. The equations are derived in four steps.

First step:
The adaptive filter output is given by

$$\begin{aligned} y(n) &= \mathbf{w}_n^T \mathbf{u}_2(n) \\ &= \sum_{k=0}^{M-1} w_k(n) u_2(n-k). \end{aligned} \tag{8}$$

The canceller output is given by

$$e(n) = d(n) - y(n) \tag{9}$$

where d denotes the desired response of the canceller. Now let us form the mean square error of the canceller output $e(n)$,

$$\epsilon^2(n) = E[(d(n) - y(n))^2] \tag{10}$$

where E denotes the mathematical expectation.

$$\begin{aligned} &\epsilon^2(n) \\ &= E[(d(n) - \sum_{k=0}^{M-1} w_k(n) u_2(n-k))^2] \\ &= E[d^2(n) - 2d(n) \sum_{k=0}^{M-1} w_k(n) u_2(n-k) \\ &\quad + \sum_{k=0}^{M-1} \sum_{l=0}^{M-1} w_k(n) w_l(n) u_2(n-k) u_2(n-l)]. \end{aligned} \tag{11}$$

$\mathbf{w}(n)$ is independent of both $\mathbf{u}_2(n)$ and $\mathbf{d}(n)$ [3]. The linearity of the mathematical expectation yields

$$\begin{aligned} &\epsilon^2(n) \\ &= E[d^2(n)] - 2 \sum_{k=0}^{M-1} w(k) E[d(n) u_2(n-k)] \\ &\quad + \sum_{k=0}^{M-1} \sum_{l=0}^{M-1} w(k) w(l) E[u_2(n-k) u_2(n-l)]. \end{aligned} \tag{12}$$

We assume that the adaptive filter operates in a stationary environment for analysis simplicity. Now we define the following functions.

$$R_{d,d}(0) = E[d^2(n)] \tag{13}$$

$$R_{u_2,d}(k) = E[d(n) u_2(n-k)] \tag{14}$$

$$R_{u_2,u_2}(k-l) = E[u_2(n-k) u_2(n-l)]. \tag{15}$$

where $R_{d,d}(0)$ is the auto-correlation function of d at lag zero, $R_{u_2,d}(k)$ the cross-correlation function of u_2 and d at lag k, $R_{u_2,u_2}(k-l)$ the auto-correlation function of u_2 at lag $k-l$.

Equation (12) can be rewritten using Eqs. (13) through (15) by

$$\begin{aligned} \epsilon^2 &= R_{d,d}(0) - 2 \sum_{k=0}^{M-1} w(k) R_{u_2,d}(k) \\ &\quad + \sum_{k=0}^{M-1} \sum_{l=0}^{M-1} w(k) w(l) R_{u_2,u_2}(k-l). \end{aligned} \tag{16}$$

The mean square error reaches its minimum when the gradient is null.

$$\begin{aligned} &\frac{\partial \epsilon^2}{\partial w(k)} = 0 \Longleftrightarrow \\ &\quad -2R_{u_2,d}(k) + 2 \sum_{l=0}^{M-1} w(l) R_{u_2,u_2}(k-l) = 0. \end{aligned} \tag{17}$$

Equation (17) yields

$$R_{u_2,d}(k) = \sum_{l=0}^{M-1} w(l) R_{u_2,u_2}(k-l). \tag{18}$$

The proof of Eq. (18) is provided in Appendix A. By taking the Fourier transform of both sides of Eq. (18) we get

$$S_{u_2,d}(j\omega) = F_A(j\omega) S_{u_2,u_2}(\omega) \tag{19}$$

where $S_{u_2,d}(j\omega)$ is the cross-power spectrum of u_2 and d, $F_A(j\omega)$ the adaptive filter frequency response after convergence, $S_{u_2,u_2}(\omega)$ the power spectrum of u_2, and ω the angular frequency.

Second step:
We will derive the canceller output power spectrum $S_{e,e}(\omega)$

$$\begin{aligned} e(n) &= d(n) - y(n) \\ &= d(n) - \sum_{l=0}^{M-1} w(l) u_2(n-l). \end{aligned} \tag{20}$$

The auto-correlation function of e(n) becomes

$$R_{e,e}(k) = E[e(n)e(n+k)] \tag{21a}$$

$$\begin{aligned} &= E[(d(n) - \sum_{l=0}^{M-1} w(l) u_2(n-l)) \\ &\quad \bullet (d(n+k) - \sum_{l=0}^{M-1} w(l) u_2(n+k-l))] \\ &= E[d(n)d(n+k)] \\ &\quad - \sum_{l=0}^{M-1} w(l) E[u_2(n-l)d(n+k)] \\ &\quad - \sum_{l=0}^{M-1} w(l) E[d(n)u_2(n+k-l)] \\ &\quad + \sum_{l=0}^{M-1} w(l) \sum_{p=0}^{M-1} w(p) \\ &\quad \bullet E[u_2(n-l)u_2(n+k-p)] \end{aligned} \tag{21b}$$

$$= R_{d,d}(k) - \sum_{l=0}^{M-1} w(l) R_{d,u_2}(k-l). \tag{21c}$$

The proof of Eq. (21c) is provided in Appendix B. The Fourier transform of Eq. (21c) gives

$$S_{e,e}(\omega) = S_{d,d}(\omega) - F_A(j\omega) S_{d,u_2}(j\omega). \tag{22}$$

Now we substitute $F_A(j\omega)$ of Eq. (19) in Eq. (22).

$$S_{e,e}(\omega) = S_{d,d}(\omega) - \frac{S_{u_2,d}(j\omega) S_{d,u_2}(j\omega)}{S_{u_2,u_2}(\omega)} \tag{23a}$$

$$= S_{d,d}(\omega) - \frac{|S_{u_2,d}(j\omega)|^2}{S_{u_2,u_2}(\omega)}. \tag{23b}$$

Third step:
We will evaluate the power spectrum of the desired response $S_{d,d}(\omega)$. The notations $s(n)$, n_0 and $u_1(n)$ are replaced in order to simplify mathematical expressions as follows:

$$x_0(n) = s(n), \quad x_1(n) = n_0(n), \quad y_1(n) = u_1(n). \tag{24}$$

Letting h_0 and h_1 be the impulse responses of the paths from the signal source to adder1 and from the noise source through filter 1 to adder2, respectively, the desired response is expressed by

$$y_0(n) = \sum_{k=1}^{\infty} h_0(k) x_0(n-k) \tag{25}$$

$$y_1(n) = \sum_{k=1}^{\infty} h_1(k) x_1(n-k) \tag{26}$$

$$\begin{aligned} d(n) &= \sum_{i=0}^{1} y_i(n) \\ &= \sum_{i=0}^{1} \sum_{l=1}^{\infty} h_i(l) x_i(n-l) \end{aligned} \tag{27}$$

Furthermore, the auto-correlation of $d(n)$ is given by

$$R_{d,d}(k) = E[d(n)d(n+k)] \tag{28a}$$

$$\begin{aligned} &= E[\sum_{i=0}^{1} \sum_{l=1}^{\infty} h_i(l) x_i(n-l) \\ &\quad \bullet \sum_{j=0}^{1} \sum_{p=1}^{\infty} h_j(p) x_j(n+k-p)] \\ &= E[\sum_{i=0}^{1} \sum_{j=0}^{1} \sum_{l=1}^{\infty} h_i(l) x_i(n-l) \\ &\quad \bullet \sum_{p=1}^{\infty} h_j(p) x_j(n+k-p)] \\ &= \sum_{i=0}^{1} \sum_{j=0}^{1} \sum_{l=1}^{\infty} \sum_{p=1}^{\infty} h_i(l) h_j(p) \\ &\quad \bullet E[x_i(n-l) x_j(n+k-p)] \\ &= \sum_{i=0}^{1} \sum_{j=0}^{1} \sum_{l=1}^{\infty} \sum_{p=1}^{\infty} h_i(l) h_j(p) \\ &\quad \bullet R_{x_i,x_j}(l+k-p). \end{aligned} \tag{28b}$$

The power spectrum of $d(n)$ is obtained as the Fourier transform of $R_{d,d}(k)$. After some transformations, we get

$$S_{d,d}(\omega) = \sum_{i=0}^{1} \sum_{j=0}^{1} H_i^*(j\omega) H_j(j\omega) S_{x_i,x_j}(j\omega) \tag{29}$$

where $*$ denotes the complex conjugate operator. The proof of Eq. (29) is provided in Appendix C. Now we apply this result to the noise canceller circuit shown in Fig. 1. In this circuit, $H_0(j\omega) = 1$, $H_1(j\omega) = F_1(j\omega)$, $S_{x_0,x_0}(\omega) = S_{s,s}(\omega)$, $S_{x_1,x_0}(j\omega) = S_{n_o,s}(j\omega)$, $S_{x_1,x_1}(\omega) = S_{n_o,n_o}(j\omega)$ where $S_{s,s}(\omega)$, $S_{n_o,s}(j\omega)$ and $S_{n_o,n_o}(\omega)$ are the power spectrum of the signal, the cross-power spectrum of the noise and the signal and the power spectrum of the noise, respectively.

2.4 SRNC Performance Based on Correlations between Signal and Noise

2.4.1 Uncorrelated Signal and Noise

Under this condition, we have

$$\begin{aligned} S_{x_i,x_j} &= 0 \quad \text{if} \quad i \neq j \\ S_{x_i,x_j} &> 0 \quad \text{if} \quad i = j. \end{aligned} \tag{30}$$

By using Eqs. (24) and (30), $S_{d,d}(\omega)$ given by Eq. (29) is expressed by

$$\begin{aligned} S_{d,d}(\omega) &= \sum_{i=0}^{1} |H_i(j\omega)|^2 S_{x_i,x_i}(\omega) \\ &= S_{s,s}(\omega) + |F_1(j\omega)|^2 S_{n_o,n_o}(\omega). \end{aligned} \tag{31}$$

Let us evaluate more explicitly $S_{u_2,d}(j\omega)$ by using a well known technique in multiple-input system [6], [7]. It is easy to show

$$S_{u_2,d}(j\omega) = S_{u_2,u_1}(j\omega). \tag{32}$$

Next, we consider the relations between $u_1(n)$ and $u_2(n)$. They are given by

$$u_2(n) = \sum_{k=0}^{\infty} h_2(k) n_o(n-k) \tag{33}$$

$$u_1(n) = \sum_{k=0}^{\infty} h_1(k) n_o(n-k) \tag{34}$$

where $h_1(n)$ and $h_2(n)$ are the impulse responses of $F_1(j\omega)$ and $F_2(n)$, respectively. By multiplying each side of above first and second previous equations by $n_o(n+\tau)$ and $u_2(n-\tau)$, respectively, and applying the expectation operator we get

$$\begin{aligned} R_{u_2,n_o}(\tau) &= E[u_2(n) n_o(n+\tau)] && \text{(35a)} \\ &= \sum_{k=0}^{\infty} E[h_2(k) n_o(n+\tau) n_o(n-k)] \\ &= \sum_{k=0}^{\infty} h_2(k) R_{n_o,n_o}(-\tau-k). && \text{(35b)} \end{aligned}$$

In the same manner, we easily show that

$$R_{u_2,u_1}(\tau) = \sum_{k=0}^{\infty} h_1(k) R_{u_2,n_o}(\tau-k). \tag{36}$$

Using auto-correlation function symmetry, substituting $R_{u_2,n_o}(\tau)$ in $R_{u_2,u_1}(\tau)$, and taking its Fourier transform, we get

$$S_{u_2,u_1}(j\omega) = F_1(j\omega) F_2(j\omega) S_{n_o,n_o}(\omega). \tag{37}$$

Next, we must to do is to rewrite $S_{e,e}(\omega)$ given by Eq. (23b) using $S_{s,s}(\omega)$ and $S_{n_o,n_o}(\omega)$. It is well known that

$$S_{u_2,u_2}(\omega) = |F_2(j\omega)|^2 S_{n_o,n_o}(\omega). \tag{38}$$

By substituting Eqs. (31) and (37) in Eq. (23b), we get

$$\begin{aligned} S_{e,e}(\omega) &= S_{s,s}(\omega) + |F_1(j\omega)|^2 S_{n_o,n_o}(\omega) \\ &\quad - S_{n_o,n_o}(\omega) |F_1(j\omega)|^2. \end{aligned} \tag{39}$$

It is well known that the auto-spectrum of a WSS (wide sense stationary) process is non negative [6]. That is,

$$|S_{n_o,n_o}(\omega)| = S_{n_o,n_o}(\omega), \tag{40}$$

then we have

$$\begin{aligned} S_{e,e}(\omega) &= S_{s,s}(\omega) + |F_1(j\omega)|^2 S_{n_o,n_o}(\omega) \\ &\quad - |F_1(j\omega)|^2 S_{n_o,n_o}(\omega) \\ &= S_{s,s}(\omega). \end{aligned} \tag{41}$$

This means that after the adaptation completely convergence, the output error does not include noise components, at the same time, the signal is not distorted.

2.4.2 Correlated Signal and Noise

By using Eq. (29),

$$\begin{aligned} S_{d,d}(\omega) &= S_{s,s}(\omega) + F_1(j\omega) S_{s,n_o}(j\omega) \\ &\quad + F_1^*(j\omega) S_{n_o,s}(j\omega) \\ &\quad + |F_1(j\omega)|^2 S_{no,n_o}(\omega). \end{aligned} \tag{42}$$

Let us evaluate more explicitly $S_{u_2,d}(j\omega)$

$$\begin{aligned} R_{u_2,d}(\tau) &= E[u_2(n)(s(n+\tau) + u_1(n+\tau))] && \text{(43a)} \\ &= E[u_2(n) s(n+\tau)] + E[u_2(n) u_1(n+\tau)] \\ &= E[\sum_{k=0}^{\infty} h_2(k) n_o(n-k) s(n+\tau)] \\ &\quad + E[u_2(n) u_1(n+\tau)] && \text{(43b)} \end{aligned}$$

$$R_{s,n_o}(\tau) = E[s(n) n_o(n+\tau)] \tag{44}$$

$$\begin{aligned} R_{u_2,d}(\tau) &= \sum_{k=0}^{\infty} h_2(k) R_{s,n_o}(\tau+k) \\ &\quad + E[u_2(n) u_1(n+\tau)]. \end{aligned} \tag{45}$$

It is well known that

$$R_{s,n_o}(-\tau) = R_{n_o,s}^*(\tau) \tag{46}$$

$$S_{n_o,s}(j\omega) = S^*_{s,n_o}(j\omega) \tag{47}$$

Furthermore, we deal with real data in the paper. The Fourier transform of both side of Eq. (41) yields

$$\begin{aligned} S_{u_2,d}(j\omega) &= S^*_{s,n_o}(j\omega)F_2(j\omega) \\ &\quad + S_{n_o,n_o}(j\omega)F_1(j\omega)F_2(j\omega) \end{aligned} \tag{48}$$

where Eq. (37) is also taken into account.

By substituting Eqs. (42) and (46) in Eq. (23b), and after some manipulations, we get

$$\begin{aligned} S_{e,e}(\omega) &= S_{s,s}(\omega) + |F_1(j\omega)|^2 S_{n_o,n_o}(\omega) \\ &\quad + F_1(j\omega)S_{s,n_o}(j\omega) + F_1^*(j\omega)S^*_{s,n_o}(j\omega) \\ &\quad - \frac{|S^*_{s,n_o}(j\omega) + S_{n_o,n_o}(\omega)F_1(j\omega)|^2}{S_{n_o,n_o}(\omega)} \end{aligned} \tag{49a}$$

$$= S_{s,s}(\omega) - \frac{|S_{s,n_o}(j\omega)|^2}{S_{n_o,n_o}(\omega)} \tag{49b}$$

In the above expression, the second term indicates effect of the cross-correlation of the signal and noise. Since the signal-noise cross-correlation produces the missing of some signal frequency components included in the noise; that is, some distortion is caused, the sign of the second term is minus. We can define the noise canceller performance by

$$P_{NC} = \frac{S_{e,e}(\omega)}{S_{s,s}(\omega)} . \tag{50}$$

Since $S_{s,n_o}(j\omega)$ is the cross-power spectrum, that is the signal-noise correlation, Eq. (49b) shows that the noise canceller performance is inversely proportional to the signal-noise correlation.

3. Computer Simulation

3.1 Noise Path Characteristics

Second-order transfer functions are employed for the noise paths F_1 and F_2.

$$F_i(z) = h_o \frac{1 - 2\rho\cos\theta z^{-1} + \rho^2 z^{-2}}{1 - 2r\cos\phi z^{-1} + r^2 z^{-2}}, \quad i = 1, 2 \tag{51}$$

F_1: $r = 0.8, \phi = \pi/4\,[\text{rad}], \rho = 1, \theta = \pi\,[\text{rad}]$
F_2: $r = 0.8, \phi = \pi/2\,[\text{rad}], \rho = 1, \theta = \pi\,[\text{rad}]$
Figure 2 shows the amplitude responses of the filters F_1 and F_2. The normalized frequency of 1 Hz indicates $f_s/2$, where f_s is a sampling frequency.

3.2 Cross-Correlation Function Computation

We have supposed that all processes used in this paper are stationary. Therefore, the cross-correlation function does not depend on time, but depends only on the time lag. The cross-correlation function $R_{s,n_o}(j\omega)$ between the signal $s(n)$ and the noise $n_o(n)$ is defined by Eq. (44) [8]. In practice, however, a finite length of the infinite length random data is only available. Therefore, the cross-correlation function must be estimated. For doing so, we must carefully set the lower and upper limits of the above series. First, the length of the cross-correlation function is evaluated as follow:

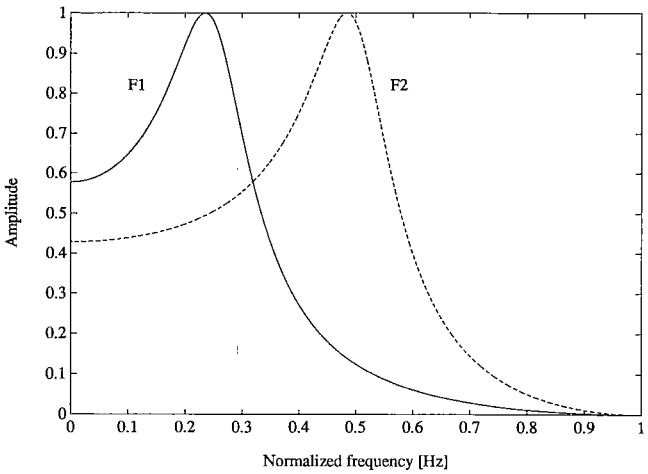

Fig. 2 Amplitude responses of F_1 and F_2.

For positive time lag, the lowest value is 0 and the largest is $(N-1)-0 = N-1$. Where N is the data length. This means $n = 0, 1, \cdots, N-1$. Then, $m \in I = [0, N-1]$. Similarly, for negative time lag, m$\in J = [1-N, 0]$. Finally, the cross-correlation function length is $2(N-1)+1 = 2N-1$. For positive lag time, we have:

$$\begin{aligned} &0 \leqq m \leqq N-1 \quad \text{and} \quad 0 \leqq n \leqq N-1 \Longrightarrow \\ &0 \leqq m+n \leqq 2N-2. \end{aligned} \tag{52}$$

Because the term $m+n$ must fall within the interval I, we have $m+n \leqq N-1$. That is $n \leqq N-m-1$. Finally, the cross-correlation function at positive lag time ($|m| = m$) is given by

$$R_{s,n_o}(m) = \frac{1}{N-m} \sum_{n=0}^{N-m-1} s(n)n_o(n+m). \tag{53}$$

For negative time lag, we have:

$$\begin{aligned} &1-N \leqq m \leqq 0 \quad \text{and} \quad 0 \leqq n \leqq N-1 \Longrightarrow \\ &1-N \leqq n+m \leqq N-1. \end{aligned} \tag{54}$$

Because the term $m+n$ must fall within the interval I, we have $0 \leqq m+n$. That is $n \geqq -m$. Finally, the cross-correlation function at negative lag time ($m < 0$) is given by

$$R_{s,n_o}(m) = \frac{1}{N-|m|} \sum_{n=-m}^{N-1} s(n)n_o(n+m) \quad m < 0. \tag{55}$$

Equations (53) and (55) are referred to as unbiased estimate of the cross-correlation function [6]. In order to show the cross-correlation function, it is shifted to the right side. Then, the time lag zero on the graph corresponds to the actual time lag $1 - N$, and the time lag N on the graph corresponds to the actual time lag zero. Finally, the time lag $2N - 2$ on the graph corresponds to the actual time lag $N - 1$.

3.3 Simulation Results

Computer simulations were carried out using real sound, multi-frequency signal and their combinations. They include, (1) Voice1/Multi-tone, (2) White noise signal/White noise, (3) Voice1/Workstation noise, (4) Voice1/Voice2, and (5) Multi-tone/White noise + one common frequency. Different SNR (signal-to-noise ratio) are investigated. The noise variance is normalized to unity. The signal and noise correlation is computed based on the unbiased estimate [8],[9]. The simulation is repeated over 2×10^4 iterations. The SNR after cancellation is evaluated using the samples from 18001 to 20000 iterations. In the simulation results show in Figs. 3 through 7, SNR before noise cancellation is chosen to be -20 dB. The adaptive filter has 20 taps. Figure 3 shows simulation results for the combination (1) Voice1/Multi-tone. A drastic reduction in the residual noise power is achieved. As shown on the graph of the cross-correlation function, at many time lag, the signal-noise cross-correlation is low.

Figure 4 shows simulation results for the combination (2) White noise signal/White noise. Since the two white noises have no correlation, noise reduction is also good. At a few time lags, the cross-correlation function takes lower value compared to the previous case.

Figure 5 shows the combination (3) Voice1/ Workstation noise. The performance is lower than the previous cases shown in Figs. 3 and 4. The cross-correlation function has higher value in average, compared to the previous cases.

In Fig. 6, the signal voice 1 is the voice of a native Japanese male and the noise voice 2 is the voice of another Japanese male telling the same sentence. The learning curve has peaks at some iterations. The cross-correlation function takes large values. This has caused

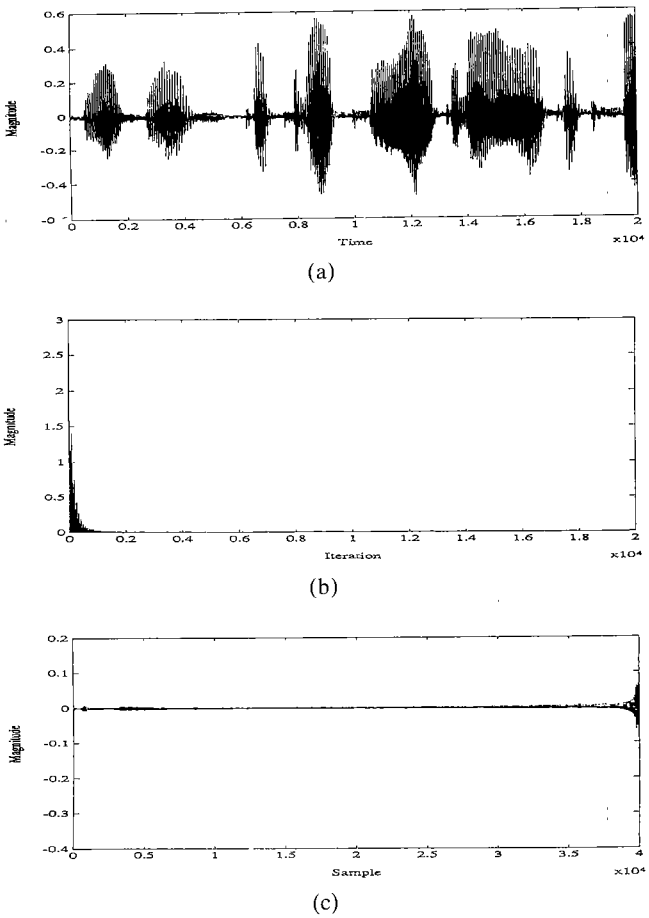

Fig. 3 Voice 1/Multi-tone. (a) Voice 1. (b) Residual noise power at the canceller output. (c) Signal and noise cross-correlation function.

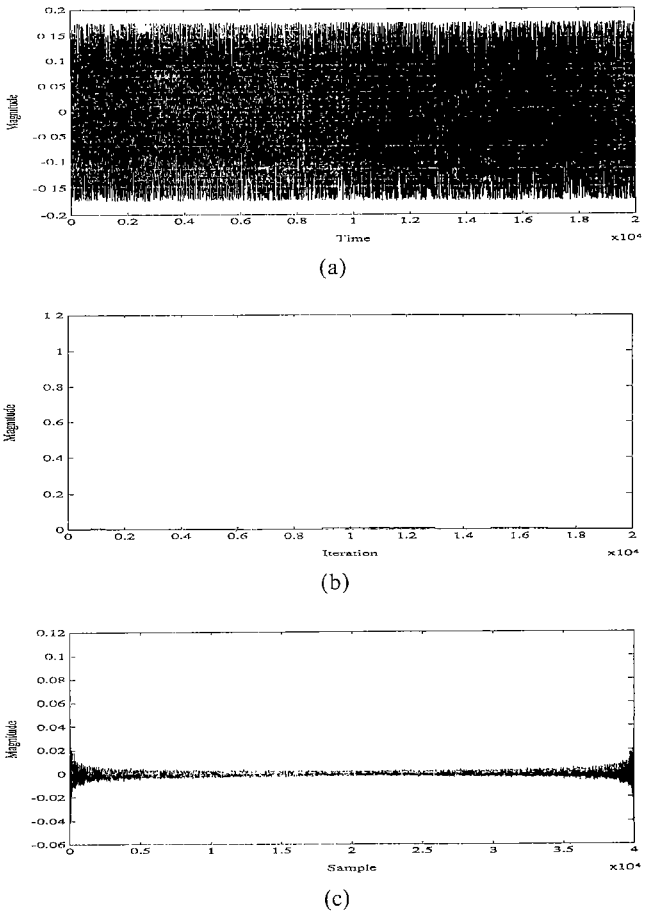

Fig. 4 White noise signal/White noise. (a) White noise signal. (b) Residual noise power at the canceller output. (c) Signal and noise cross-correlation function.

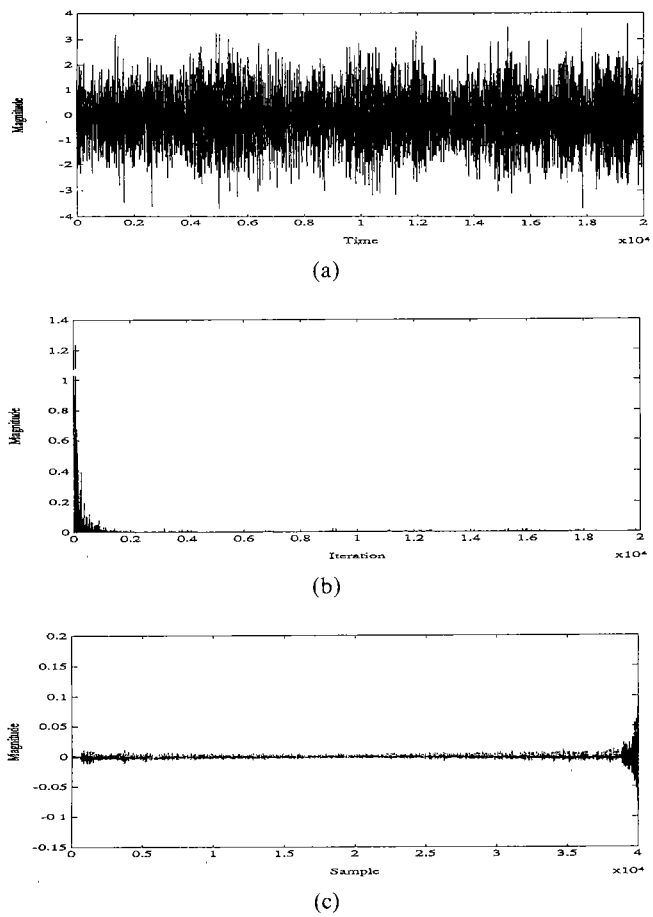

Fig. 5 Voice 1/Workstation noise. (a) Workstation noise. (b) Residual noise at the canceller output. (c) Signal and noise cross-correlation function.

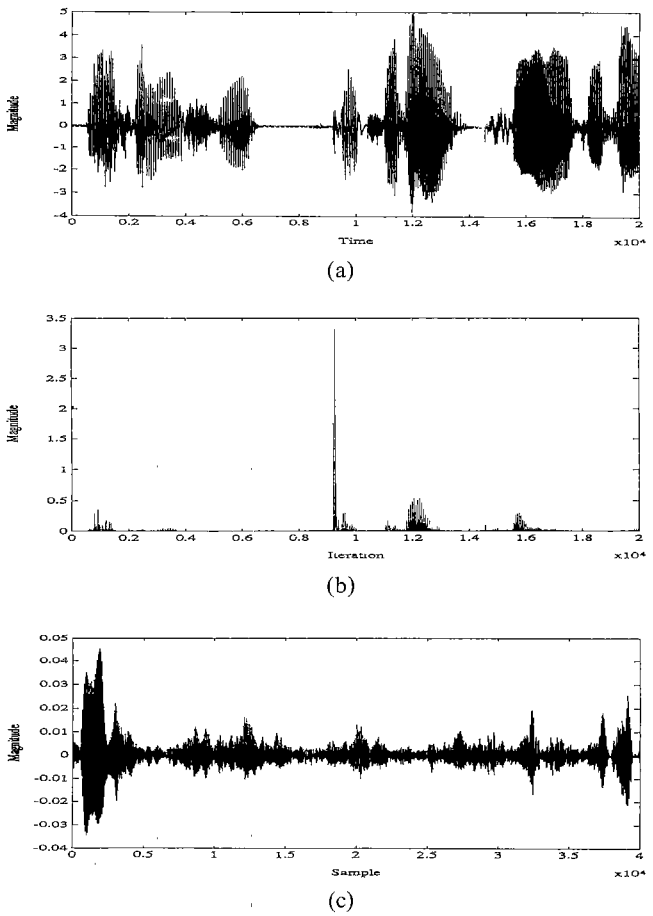

Fig. 6 Voice 1/Voice 2. (a) Voice 2. (b) Residual noise power at the canceller output. (c) Signal and noise cross-correlation function.

the peaks of the learning curve.

Figure 7 shows simulation results for the combination multi-tone signal/white noise + one common frequency. The signal frequency, which is also included in the noise, is the lowest one. The line spectra of the canceller output shows the missing of that common frequency. Thus, the signal frequency included in the noise is canceled. This causes the signal waveform distortion. The cross-correlation function takes higher values compared to all the previous cases. The impulse due to the auto-correlation of the white noise is buried in the sine wave.

Table 1 establishes the relation between noise canceller performance and the signal-noise correlation. In this table, *SNR1* is SNR before noise cancellation, *SNR2* after noise cancellation, and *DELTA*, the difference between *SNR2* and *SNR1*, that is the improvement in *SNR*. The cross-correlation mean *(CCM)* is calculated by averaging the absolute value of the cross-correlation function.

Figure 8 illustrates Table 1. The horizontal axis is a semilogarithmic scale. It defines the signal-noise correlation which is calculated by averaging the absolute value of the cross-correlation function. That is, the signal and noise correlation is actually *CCM*. Mathematical definition of *CCM*:

$$CCM = \frac{1}{2N-1} \sum_{m=0}^{m=2N-2} |R_{s,n_o}(m)|. \tag{56}$$

The vertical axis defines (a) SNR2 and (b) DELTA. As shown in Fig. 8, the noise canceller performance is inversely proportional to the signal-noise correlation. These results are supported by the theoretical analysis in Sect. 2.

4. Multi-Reference Noise Canceller

4.1 Block Diagram

The signal is generated from a single source. The noises are generated from several sources. Figure 9 shows a block diagram of the multi-reference noise canceller *(MRNC)* [1], [2], which includes two noise sources. F_{ij}, $i = 1, 2$, $j = 1, 2, 3$ represent noise paths from the

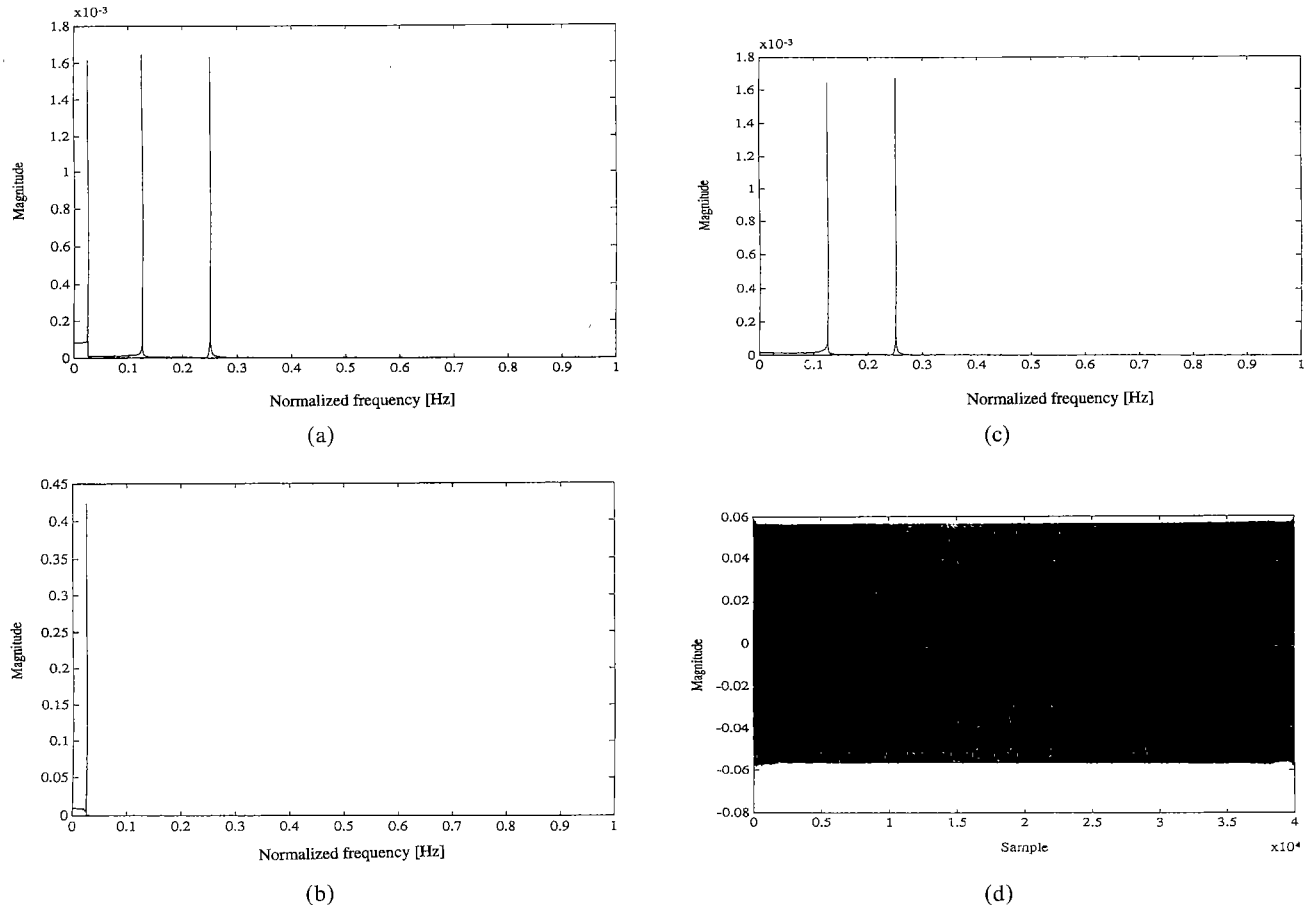

Fig. 7 Multi-tone signal/White noise + one common frequency. (a) Signal last 2000 samples power spectrum. (b) Noise last 2000 samples power spectrum. (c) Canceller output last 2000 samples power spectrum. (d) Signal and noise cross-correlation function.

Table 1 Relations between noise cancellation and signal-noise cross-correlation using different SNRs.

Combination / SNR1	Voice1/ Multitone	White noise/ White noise	Voice1/Work station noise	Voice1/ Voice2	Multitone/White noise+ one common frequency
−20 dB	CCM = 0.0010 SNR2 = 22 Delta = 42	CCM = 0.0018 SNR2 = 18 Delta = 38	CCM = 0.0021 SNR2 = 15 Delta = 37	CCM = 0.0031 SNR2 = 9 Delta = 29	CCM = 0.0287 SNR2 = 4 Delta = 24
−10 dB	CCM = 0.0032 SNR2 = 22 Delta = 32	CCM = 0.0057 SNR2 = 19 Delta = 29	CCM = 0.0067 SNR2 = 17 Delta = 27	CCM = 0.0098 SNR2 = 9 Delta = 19	CCM = 0.0906 SNR2 = 4 Delta = 14
0 dB	CCM = 0.0100 SNR2 = 24 Delta = 24	CCM = 0.0179 SNR2 = 21 Delta = 21	CCM = 0.0210 SNR2 = 20 Delta = 20	CCM = 0.0310 SNR2 = 10 Delta = 10	CCM = 0.2865 SNR2 = 4 Delta = 4
+10 dB	CCM = 0.0317 SNR2 = 28 Delta = 18	CCM = 0.0565 SNR2 = 27 Delta = 17	CCM = 0.0663 SNR2 = 23 Delta = 13	CCM = 0.0981 SNR2 = 10 Delta = 0	CCM = 0.9061 SNR2 = 4 Delta = −6
+20 dB	CCM = 0.1001 SNR2 = 30 Delta = 10	CCM = 0.1786 SNR2 = 29 Delta = 9	CCM = 0.2096 SNR2 = 24 Delta = 4	CCM = 0.3102 SNR2 = 9 Delta = −11	CCM = 2.8653 SNR2 = 4 Delta = −16

SNR1: Signal-To-Noise ratio before cancellation; SNR2: Signal-To-Noise ratio after cancellation; CCM: Croos-correlation mean; Delta = SNR2 −SNR1.

noise sources 1 and 2 to the adders 1, 2 and 3, respectively. The noises $n_1(n)$ and $n_2(n)$ are added to the signal through F_{11} and F_{21} at Add1, resulting in $d(n)$. It is assumed that the noises $n_1(n)$ and $n_2(n)$ can be detected by Add2 and Add3. The outputs from these adders, $u_1(n)$ and $u_2(n)$, are used to generate a replica

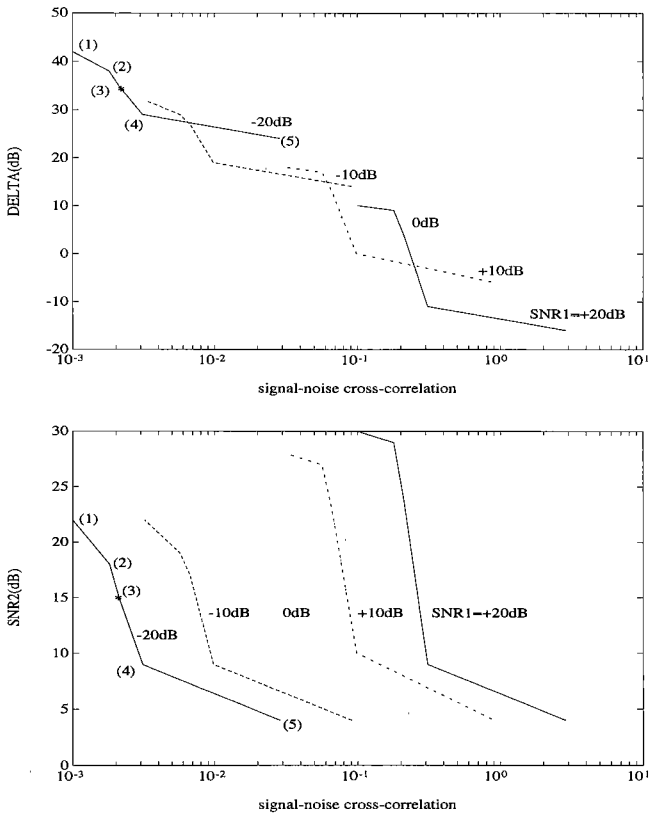

Fig. 8 Signal-noise cross-correlation and NLMS performance. (a) Cross-correlation and DELTA relation. (b) Cross-correlation and SNR2 relation.

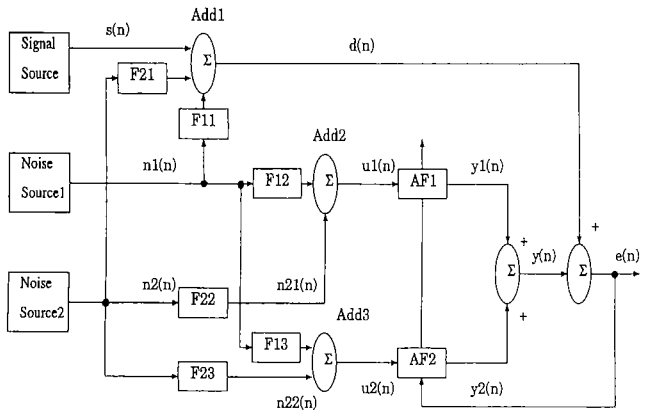

Fig. 9 Block diagram of multi-reference noise canceller.

of the noises mixed with the signal. Two FIR transversal adaptive filters, AF_1 and AF_2 with M tap-weights, are employed. The adaptive filters tap-weights are adjusted using the NLMS algorithm.

Optimum transfer functions of the adaptive filters can be obtained by setting $e(n)$ to be equal to $s(n)$ in the block diagram shown in Fig. 9. First the following condition is derived.

$$N_1(z)[F_{11}(z) - AF_{1opt}(z)F_{12}(z) - AF_{2opt}(z)F_{13}(z)] + N_2(z)[F_{21}(z) - AF_{1opt}(z)F_{22}(z) - AF_{2opt}(z)F_{23}(z)] = 0 \quad (57)$$

where $AF_{1opt}(z)$ and $AF_{2opt}(z)$ denote the optimum transfer functions of the adaptive filters 1 and 2, respectively. Under the assumption that noise1 and noise2 are uncorrelated, that is independent to each other, Eq. (64) is true, if and only if the coefficient terms of $N_1(z)$ and $N_2(z)$ are null. That is,

$$F_{11}(z) - AF_{1opt}(z)F_{12}(z) - AF_{2opt}(z)F_{13}(z) = 0 \quad (58)$$

$$F_{21}(z) - AF_{1opt}(z)F_{22}(z) - AF_{2opt}(z)F_{23}(z) = 0. \quad (59)$$

Solving these equations yields

$$AF_{1opt}(z) = \frac{F_{11}(z)F_{23}(z) - F_{21}(z)F_{13}(z)}{F_{12}(z)F_{23}(z) - F_{13}(z)F_{22}(z)} \quad (60)$$

$$AF_{2opt}(z) = \frac{F_{12}(z)F_{21}(z) - F_{11}(z)F_{22}(z)}{F_{12}(z)F_{23}(z) - F_{13}(z)F_{22}(z)}. \quad (61)$$

4.2 Computer Simulation

4.2.1 Noise Path Characteristics:

As shown in Eqs. (60) and (61), the optimum adaptive filters $AF_{1opt}(z)$ and $AF_{2opt}(z)$ are rational functions of z^{-1}, which includes poles. Unstable poles in the optimum $AF_{1opt}(z)$ and $AF_{2opt}(z)$ are avoided in the simulation. Because this problem is not a point we are discussing in this paper. The noise path transfer functions are given by second-order functions as shown in Eq. (51), and the parameters are given by

$F_{11}(z)$: Unity, $F_{12}(z)$: Unity,
$F_{13}(z)$: Unity, $F_{21}(z)$: Unity
$F_{22}(z)$: $r = 0.8$, $\phi = \pi/4$ [rad],
$\rho = 1$, $\theta = \pi$ [rad]
$F_{23}(z)$: $r = 0.8$, $\phi = 3\pi/2$ [rad],
$\rho = 1$, $\theta = \pi/2$ [rad]

Figure 10 shows the amplitude responses of $F_{22}(z)$ and $F_{23}(z)$.

4.2.2 Simulation Results

The signal source $s(n)$ generates a speech signal. Noise sources $n_1(n)$ and $n_2(n)$ generate white noise and workstation noise, respectively. The following combinations are considered. The combinations of speech signal and two noises, which include White noise & Single tone 1 and White noise & Single tone 2. SNR1 equals 0 dB and each adaptive filter has 20 taps. Table 2 shows the results. The tones 1 and 2 contain 5 frequencies. From Table 2, the lower is the tone frequency component, the worse is the cancellation. This result can be explained as follows: Of course, speech spectrum mainly concentrates at low frequencies as shown in Fig. 11; then, when

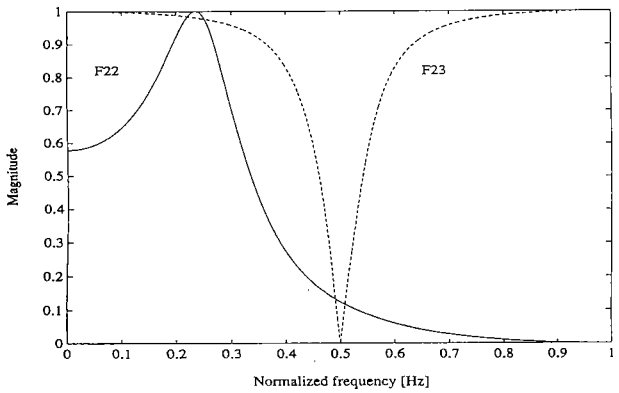

Fig. 10 Amplitude responses of noise paths $F_{22}(z)$ and $F_{23}(z)$.

Table 2 Tones 1 and 2 frequencies and SNR2 relation. (SNR1 = 0 dB)

f1 [KHz] / f2 [KHz]	0.1	0.2	0.3	1	3.8
0.1	SNR2= 10 dB	13	14	14	14
0.2	11	13	16	18	19
0.3	12	14	16	20	22
1	13	17	20	21	23
3.8	12	15	18	22	26

f1: Tone 1 frequency; f2: Tone 2 frequency.

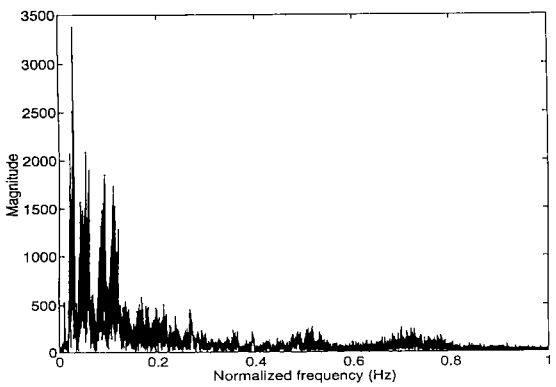

Fig. 11 Speech signal spectrum.

the tone approaches the low band, its correlation with the speech increases.

Table 3 shows effects of the number of taps on the noise cancellation. The combination Speech signal/White noise/Workstation noise is considered. SNR1 equals 0 dB. For 20 taps, the improvement is 15 dB. This is lower than 20 dB obtained in *SRNC* for the combination of Speech and Workstation noise shown in Table 1. As a matter of fact, MRNC is more sensitive to cross-correlation than SRNC. Moreover, when the number of adaptive filter taps is increased, *SNR2* is reduced. This means that by increasing the number of filter taps, the noise components included in the signal are more precisely canceled.

Table 3 SNR2 after noise cancellation by adjusting the adaptive filters of M taps. (SNR1 = 0 dB)

M	20	50	100	200	400	800	2000	2500
SNR2 (dB)	15	15	14	12	9	7	5	5

5. Conclusion

Single-Reference and Multi-Reference noise canceller performances have been investigated based on the correlation between the signal and the noises. For SRNC, the simulation results have shown that the performance is inversely proportional to the signal-noise correlation as expected by the theoretical analysis. High correlation between the signal and the noise causes significant signal waveform distortion. For MRNC, the same relation is held. However, it is more sensitive to the signal-noise cross-correlation than that of SRNC.

References

[1] B. Widrow, et al, "Adaptive noise cancelling: Principles and applications," Proc. IEEE, vol.63, no.12, pp.1692–1716, Dec. 1975.
[2] B. Widrow and D. Stearns, "Adaptive Signal Processing," Prentice-Hall, 1985.
[3] S. Haykin, "Adaptive Filter Theory," Second ed., Prentice Hall, 1991.
[4] Y. Atse, Z. Ma, and K. Nakayama, "Analysis of NLMS noise canceller performance based on correlation between signal and noise," IEICE Technical Report, vol.92, no.430, DSP92-95, pp.79–86, Jan. 1993.
[5] Y. Atse, Z. Ma, and K. Nakayama, "Performance of NLMS noise canceller based on correlation between signal and noise," International Workshop on Intelligent Signal Processing, Sendai, Japan, pp.345–349, Oct. 1993.
[6] S. Bendat and G. Piersol, "Random Data Analysis and Measurement Procedures," Wiley-Interscience, 1971.
[7] A. Papoulis, "Probability, Random Variables, and Stochastic Processes," Second ed., McGraw-Hill, 1984.
[8] J.N. Little and L. Shure, "Matlab Signal Processing Toolbox," The Math Works, Inc., 1988.
[9] S. Bendat and G. Piersol, "Engineering Applications of Correlation and Spectral Analysis," Wiley-Interscience, 1993.

Appendix A: Proof of Equation (18)

Here we recall Eq. (18) as a matter of convenience.

$$R_{u_2,d}(k) = \sum_{l=0}^{M-1} w(l) R_{u_2,u_2}(k-l). \qquad (A\cdot 1)$$

Let us consider Eq. (16) given by

$$\epsilon^2 = R_{d,d}(0) - 2\sum_{k=0}^{M-1} w(k) R_{u_2,d}(k) + \sum_{k=0}^{M-1}\sum_{l=0}^{M-1} w(k)w(l) R_{u_2,u_2}(k-l). \qquad (A\cdot 2)$$

The mean square error reaches its minimum when the gradient is mull; that is,

$$\frac{\partial \epsilon^2}{\partial w(k)} = 0. \tag{A·3}$$

We will prove by the recursive method.

a) For $M = 1$ (The adaptive filter has one tap). Equation (16) gives

$$\epsilon^2 = R_{d,d}(0) - 2w(0)R_{u_2,d}(0) + w^2(0)R_{u_2,u_2}(0) \tag{A·4}$$

$$\frac{\partial \epsilon^2}{\partial w(0)} = -2R_{u_2,d}(0) + 2w(0) + 2w(0)R_{u_2,u_2}(0) = 0 \tag{A·5}$$

$$\Longrightarrow R_{u_2,d}(0) = w(0)R_{u_2,u_2}(0) \tag{A·6}$$

$$M = 1 \Longrightarrow k = 0 \Longrightarrow$$

$$R_{u_2,d}(k) = \sum_{l=0}^{0} w(l)R_{u_2,u_2}(k-l). \tag{A·7}$$

Then Eq. (18) is true for one tap.

b) We suppose that Eq. (17) is true for M tap-weights, and will show that it is true for $(M+1)$ taps. We recall Eq. (17).

$$\frac{\partial \epsilon^2}{\partial w(k)} = -2R_{u_2,d}(k) + 2\sum_{l=0}^{M-1} w(l)R_{u_2,u_2}(k-l). \tag{A·8}$$

For $(M+1)$ taps, Eq. (16) gives

$$\epsilon^2 = R_{d,d}(0) - 2\sum_{k=0}^{M} w(k)R_{u_2,d}(k) + \sum_{k=0}^{M}\sum_{l=0}^{M} w(k)w(l)R_{u_2,u_2}(k-l) \tag{A·9}$$

$$= R_{d,d}(0) - 2\sum_{k=0}^{M-1} w(k)R_{u_2,d}(k) - 2w(M)R_{u_2,d}(M) + \sum_{k=0}^{M}\sum_{l=0}^{M} w(k)w(l)R_{u_2,u_2}(k-l) \tag{A·10}$$

$$= R_{d,d}(0) - 2\sum_{k=0}^{M-1} w(k)R_{u_2,d}(k) + \sum_{k=0}^{M-1}\sum_{l=0}^{M-1} w(k)w(l)R_{u_2,u_2}(k-l) + \sum_{k=0}^{M-1} w(k)w(M)R_{u_2,u_2}(k-M) + \sum_{l=0}^{M-1} w(M)w(l)R_{u_2,u_2}(M-l) + w^2(M)R_{u_2,u_2}(0) - 2w(M)R_{u_2,d}(M) \tag{A·11}$$

$$= \left[R_{d,d}(0) - 2\sum_{k=0}^{M-1} w(k)R_{u_2,d}(k) + \sum_{k=0}^{M-1}\sum_{l=0}^{M-1} w(k)w(l)R_{u_2,u_2}(k-l)\right] + 2\sum_{k=0}^{M-1} w(k)w(M)R_{u_2,u_2}(k-M) + w^2(M)R_{u_2,u_2}(0) - 2w(M)R_{u_2,d}(M) \tag{A·12}$$

As we see, the term in the bracket is nothing that Eq. (16). Now we take the partial derivative of Eq. (A·12). We have supposed that Eq, (17) is true for M taps. So for $k = 0, 1, 2, \cdots M-1$, we have

$$\frac{\partial \epsilon^2}{\partial w(k)} = -2R_{u_2,d}(k) + 2\sum_{l=0}^{M-1} w(l)R_{u_2,u_2}(k-l) + 2w(M)R_{u_2,u_2}(k-M) \tag{A·13}$$

$$= 2\sum_{l=0}^{M} w(l)R_{u_2,u_2}(k-l) - 2R_{u_2,d}(k). \tag{A·14}$$

For $k = M$, we see that the term in the bracket has no contribution in the derivative. That is, we have

$$\frac{\partial \epsilon^2}{\partial w(M)} = 2\sum_{k=0}^{M-1} w(k)R_{u_2,u_2}(k-M) + 2w(M)R_{u_2,u_2}(0) - 2R_{u_2,d}(M) \tag{A·15}$$

$$= -2R_{u_2,d}(M) + 2\sum_{k=0}^{M} w(k)R_{u_2,u_2}(M-k). \tag{A·16}$$

Then, Eq. (17) is true for all $k = 0, 1, 2, \cdots M$, that is for $(M+1)$ taps. Now we only have to set

$$\frac{\partial \epsilon^2}{\partial w(k)} = 0. \tag{A·17}$$

That ends the proof of Eq. (18).

Appendix B: Proof of Equation (21c)

Here we recall Eq. (21c) as a matter of convenience.

$$R_{e,e}(k) = R_{d,d}(k) - \sum_{l=0}^{M-1} w(l)R_{d,u_2}(k-l). \tag{A·18}$$

Let us recall the following equation, that is Eq. (21b).

$$R_{e,e}(k) = E[d(n)d(n+k)]$$

$$- \sum_{l=0}^{M-1} w(l)E[u_2(n-l)d(n+k)]$$
$$- \sum_{l=0}^{M-1} w(l)E[d(n)u_2(n+k-l)]$$
$$+ \sum_{k=0}^{M-1} w(k) \sum_{l=0}^{M-1} w(l)$$
$$\bullet E[u_2(n-l)u_2(n+k-l)]. \quad \text{(A·19)}$$

Now we replace the expectations by the autocorrelations and cross-correlations functions.

$$R_{e,e}(k) = R_{d,d}(k) - \sum_{l=0}^{M-1} w(l)R_{u_2,d}(k+l)$$
$$- \sum_{l=0}^{M-1} w(l)R_{u_2,d}(l-k)$$
$$+ \sum_{l=0}^{M-1} w(l) \sum_{p=0}^{M-1} w(p)$$
$$\bullet R_{u_2,u_2}(k-p+l). \quad \text{(A·20)}$$

Now to prove Eq. (21c), it suffices to shows that the following expression is null.

$$- \sum_{l=0}^{M-1} w(l)R_{u_2,d}(k+l)$$
$$+ \sum_{l=0}^{M-1} w(l) \sum_{p=0}^{M-1} w(p)R_{u_2,u_2}(k-p+l). \quad \text{(A·21)}$$

From Eq. (18), we write

$$\sum_{p=0}^{M-1} w(p)R_{u_2,u_2}(k-p+l) = R_{u_2,d}(k+l). \quad \text{(A·22)}$$

Equation (A·21) becomes

$$- \sum_{l=0}^{M-1} w(l)R_{u_2,d}(k+l)$$
$$+ \sum_{l=0}^{M-1} w(l)R_{u_2,d}(k+l) = 0. \quad \text{(A·23)}$$

$R_{e,e}(k)$ becomes

$$R_{d,d}(k) - \sum_{l=0}^{M-1} w(l)R_{u_2,d}(l-k). \quad \text{(A·24)}$$

It is well known that for WSS processes,

$$R_{u_2,d}(l-k) = R^*_{d,u_2}(k-l). \quad \text{(A·25)}$$

Furthermore, here we deal with real data, then,

$$R^*_{d,u_2}(k-l) = R_{d,u_2}(k-l). \quad \text{(A·26)}$$

Finally, $R_{e,e}(k)$ becomes

$$R_{e,e}(k) = R_{d,d}(k) - \sum_{l=0}^{M-1} w(l)R_{d,u_2}(k-l). \quad \text{(A·27)}$$

Appendix C: Proof of Equation (29)

Here we recall Eq. (29) as a matter of convenience.

$$S_{d,d}(w) = \sum_{i=0}^{1} \sum_{j=0}^{1} H_i^*(w)H_j^*(w)S_{x_i,X_j}(w). \quad \text{(A·28)}$$

We write the following previous expression of $R_{d,d}(k)$; that is Eq. (28b).

$$R_{d,d}(k) = \sum_{i=0}^{1} \sum_{j=0}^{1} \sum_{l=1}^{\infty} \sum_{p=1}^{\infty} h_i(l)h_j(p)R_{x_i,x_j}(l+k-p). \quad \text{(A·29)}$$

The power spectrum $S_{d,d}(w)$ is the Fourier transform of $R_{d,d}(k)$. That is,

$$S_{d,d}(w) = \sum_{k=-\infty}^{\infty} \exp(-jwkT)R_{d,d}(k) \quad \text{(A·30)}$$

where $1/T$ is a sampling frequency.

$$S_{d,d}(w) = \sum_{k=-\infty}^{\infty} \exp(-jwkT)$$
$$\sum_{i=0}^{1} \sum_{j=0}^{1} \sum_{l=1}^{\infty} \sum_{p=1}^{\infty} h_i(l)$$
$$\bullet h_j(p)R_{x_i,x_j}(k+l=p). \quad \text{(A·31)}$$

Now we insert in the precedent expression, the term $\exp(-jw(p-l)T)\exp(+jw(p-l)T) = 1$. Then, that precedent expression becomes

$$S_{d,d}(w) = \sum_{i=0}^{1} \sum_{j=0}^{1} \sum_{k=-\infty}^{\infty} \sum_{l=1}^{\infty} \sum_{p=1}^{\infty} h_i(l)$$
$$\bullet \exp(jwlT)h_j(p)\exp(-jwpT)$$
$$\bullet R_{x_i,x_j}(k+l-p)$$
$$\bullet \exp(-jw(l-p+k)T). \quad \text{(A·32)}$$

Now we set $l-p+k=\tau$

$$S_{d,d}(w) = \sum_{i=0}^{1} \sum_{j=0}^{1} \sum_{l=1}^{\infty} h_i(l)\exp(jwlT)$$
$$\sum_{p=1}^{\infty} h_j(p)\exp(-jwpT)$$
$$\sum_{\tau=-\infty}^{\infty} R_{x_i,x_j}(\tau)\exp(-jw\tau T). \quad \text{(A·33)}$$

Here we recognize the Fourier transform of h and R_{x_i,x_j}, then,

$$S_{d,d}(w) = \sum_{i=0}^{1} \sum_{j=0}^{1} H_i^*(w) H_j(w) S_{x_i,x_j}(w). \quad \text{(A·34)}$$

That ends the proof of Eq. (29).

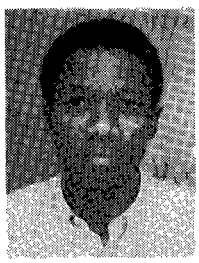

Yapi Atse has studied in undergraduate course from 1981 to 1983 and got certificate of mathematics and physics in June 1983 at university d'ABIDJAN. He obtained the degree of Ingenieur de Speciafite Telecommunications in Ecole National Superieure des Telecommunications d'ABIDJAN in June 1985. From June 1985 to October 1985, He was in France at CIT ALCATEL. From October 1985 to April 1991, he was with Ofhce National des Telecommunications de C ô te D'Ivoire. From October 1991, he has been enrolled in the doctoral course of Kanazawa university. His research interests include digital signal processing and adaptive filtering.

Kenji Nakayama received the B.E. and Dr. degrees in electronics engineering from Tokyo Institute of Technology (TIT), Tokyo, Japan, in 1971 and 1983, respectively. From 1971 to 1972 he was engaged in the research on classical network theory in TIT. He was involved in NEC Corporation from 1972 to 1988, where his research subjects were filter design methodology and signal processing algorithms. He joined the Department of Electrical and Computer Engineering at Kanazawa University, in Aug. 1988, where he is currently a Professor. His current research interests include neural networks and adaptive filters.

Zhiqiang Ma received the B.S., M.S. degrees from Dept. of Automatic Control, Central South University of Technology, China, in 1975 and 1982, respectively. She received the Ph.D. degree in 1991, from Dept. of Natural Science, Kanazawa University, Japan. She was with the Hunan Microwave Communication Company (1975–79), Central South University of Technology (1982–86), Fukui Institute of Technology (1986–87), and C & C Systems Research Laboratories, NEC Corp (1991–92). Since 1992, she has been a lecturer in Dept. of Electrical and Computer Engineering, Kanazawa University. Her current research interests include digital signal processing, adaptive filtering and neural networks. She is a member of IEEE.